Proc. Natl. Acad. Sci. USA
Vol. 94, pp. 12688–12693, November 1997
Neurobiology

Degeneration of neurons, synapses, and neuropil and glial activation in a murine *Atm* knockout model of ataxia–telangiectasia

RODRIGO O. KULJIS*†, YANG XU‡§, M. CECILIA AGUILA*, AND DAVID BALTIMORE§

*Laboratory of Brain Development, Modifiability and Neurodegenerative Disorders, Division of Behavioral Neurology, Department of Neurology, University of Miami, and Neurology Service and Geriatric Research and Education Center, Department of Veterans Affairs Medical Center at Miami, 1150 N.W. 14th Street, Suite 700, Miami, FL 33136-2115; ‡Department of Biology, University of California, San Diego, 9500 Gilman Drive, La Jolla, CA 92093-0322; and §Department of Biology, Massachusetts Institute of Technology, Cambridge, MA 02139

Contributed by David Baltimore, September 12, 1997

ABSTRACT **Neural degeneration is one of the clinical manifestations of ataxia–telangiectasia, a disorder caused by mutations in the Atm protein kinase gene. However, neural degeneration was not detected with general purpose light microscopic methods in previous studies using several different lines of mice with disrupted *Atm* genes. Here, we show electron microscopic evidence of degeneration of several different types of neurons in the cerebellar cortex of 2-month-old *Atm* knockout mice, which is accompanied by glial activation, deterioration of neuropil structure, and both pre- and postsynaptic degeneration. These findings are similar to those in patients with ataxia–telangiectasia, indicating that *Atm* knockout mice are a useful model to elucidate the mechanisms underlying neurodegeneration in this condition and to develop and test strategies to palliate and prevent the disease.**

Ataxia–telangiectasia (A-T) is typically a progressive degenerative condition that results in major neurological disability (1, 2). Death occurs frequently by the second or third decade of life from sinopulmonary infections and lymphoid tissue tumors (3–5). The frequency of A-T in the United States and Britain has been estimated to be between 1:40,000 and 1:100,000, reflecting a carrier frequency of 0.5–1% (6). Unfortunately, no effective treatments have been found to alter the course of this disease. Neurological manifestations include postural instability of the trunk as early as 1 year of age, progressing to dystonic posturing, dysmetric saccades, blinking before gaze changing, and an unusual temper tantrum (7). Later manifestations include progressive cerebellar ataxia, oculocutaneous telangiectases, choreoathetosis, oculomotor apraxia, microcephaly, progressive apathy, drooling and dysarthria, hypotonia, absent plantar responses, diffusely decreased muscle bulk due to neurogenic atrophy, progressive decline in cognitive performance, and a high propensity to neural tumors such as astrocytoma and medulloblastoma (5, 8).

In over 40 cases of A-T, necropsy has shown that there is atrophy of all cerebellar cortical layers with extensive Purkinje and granule cell loss, dentate and olivary nuclei atrophy, neuronal loss in the substantia nigra and oculomotor nuclei, spinal cord atrophy, and degenerative changes in spinal motor neurons and dorsal root and sympathetic motor neurons (9–11). Little is known, however, about the precise brain circuitry undermined by A-T, and much less is known about the exact pathophysiological mechanisms mediating the degeneration of these circuits. In addition, it is very likely that the neuropathology uncovered so far in A-T reflects a mixture of the primary neural insult plus its own progression, with an added component derived from protracted systemic complications that also cause brain alterations. The latter may well include hypoxic–ischemic brain injury caused by recurrent respiratory infections and the direct (e.g., brain metastases) and possibly even paraneoplastic effects of tumors, making it impossible to determine precisely which lesions are the primary ones, i.e., caused exclusively by the direct effect of the A-T mutation in the brain. Effective means of addressing these problems were unavailable until recently, given the obvious difficulties in obtaining large enough numbers of brain specimens, including samples throughout the course of a disease that often spans 2 or more decades.

The identification of a consistent mutation in the Atm gene in A-T patients (12) led to the generation of *Atm* knockout mice, which have been found to replicate some of the immune and neoplastic manifestations of A-T (13–15). We thus hoped that the knockout mice would also replicate the neurological manifestations of A-T, but the general purpose light microscopic histological analyses in the brains of *Atm* knockout mice published so far have failed to detect any lesions. To address this problem, we are analyzing the brains of *Atm* mice further to determine whether they exhibit any cytological, biochemical, or molecular lesions and to what extent the putative lesions may resemble those in patients with A-T. We report here on the initial phase of this project using electron microscopy, with which we have found neuronal and glial alterations indicating that *Atm* knockout mice undergo a neurodegenerative process. These observations imply that these new models of A-T may prove helpful in elucidating the pathophysiological mechanisms underlying neurodegeneration in this condition.

MATERIALS AND METHODS

Six mice [three knockouts (*Atm* −/−) and three age-matched controls] were used as experimental subjects. Because *Atm* −/− mice invariably develop thymic lymphomas and die from them by 4 months of age (13), the mice were analyzed at 2 months of age. This interval was chosen to maximize the opportunities for neurodegenerative events to occur postnatally while minimizing the possibility that advanced systemic neoplasm and paraneoplastic phenomena had a significant impact on cerebral and cerebellar structure and function. An overdose of sodium Nembutal (100 mg/Kg) was given i.p., and, after verifying the absence of brain stem reflexes, the root of the aorta was cannulated through the left ventricle. After a brief flush with 0.9% NaCl, the animals were fixed by perfusion of ≈200 ml of 2.5% paraformaldehyde plus 2.5% glutaraldehyde in 0.1 M phosphate buffer (pH 7.4) at 4°C. The brains

The publication costs of this article were defrayed in part by page charge payment. This article must therefore be hereby marked "*advertisement*" in accordance with 18 U.S.C. §1734 solely to indicate this fact.

Abbreviation: A-T, ataxia–telangiectasia.

†To whom reprint requests should be addressed. e-mail: rkuljis@mednet.med.miami.edu.

Table 1. Number of normal and abnormal granule cells, Purkinje neurons, and molecular layer neurons in both control and knockout specimens

	Granule cells		Purkinje neurons		Molecular layer neurons	
	Normal	Abnormal	Normal	Abnormal	Normal	Abnormal
Control	973	3 (0.3)	65	1 (1.5)	98	0
Knockout	679	180 (21)	66	33 (33)	77	67 (46.5)

The percentages of abnormal cells for each category of neuron, in both knockouts and controls, are shown in parentheses.

were removed with rongeurs and postfixed in the above fixative for 6 h at 4°C. Sections of the brain were obtained in the coronal or sagittal plane at 50 μm intervals using a vibratome, then embedded in Epon and appropriate areas for ultramicrotomy selected under a light microscope. Ultrathin sections were obtained at 60- to 90-nm intervals (silver–gold interference colors) and mounted on either formvar-coated slotted grids or uncoated 50- to 100-mesh grids. Some of these sections were stained with lead citrate, and the material was analyzed in a Philips Electronic Instruments (Mahwah, NJ) 300 electron microscope at an accelerating voltage of 60–80 KV as described (16, 17).

Electron micrographs of material suspected to have abnormalities in *Atm* knockout mice were compared with micrographs of equivalent material from controls and with results from well recognized publications on the normal ultrastructure of cerebellar neurons and glial cells (18–20).

To estimate the significance of the abnormalities found in knockout mice, counts of abnormal vs. normal neuronal profiles were undertaken in both experimental and control animals (Table 1). Neurons selected for counting bore the ultrastructural features of granule cells, Purkinje cells, and neurons in the molecular layer, thus providing a convenient screening for some key components of the three principal layers of the cerebellar cortex. Profiles counted were only those encountered in rasterized "sweeps" throughout the entire extent of the entire width of each layer in individual ultrathin sections, selected at regular intervals from among 63 grids with an average of three sections each. Profiles in adjacent sections and in adjacent grids were not counted to avoid sampling the same cells repeatedly and thus compromising the validity of the counting procedure. Profiles at the edge of tissue sections, within folds, cracks, and other artifacts that could interfere with their reliable identification as normal or abnormal, were not included in the counts. Because many degenerating profiles were included in such counts and given that pathological processes may alter the normal ultrastructural features of neurons and nonneuronal cells, the identification of degenerating elements as belonging to one or another cell type is necessarily tentative and based purely on comparisons with normal cells.

RESULTS

The present analysis was restricted to the cerebellar cortex because A-T affects the cerebellum most severely and because we wished to establish rapidly the relevance of any lesions that could be found in *Atm* knockout mice. We are aware, however, that analysis of other mouse brain regions will eventually be necessary to determine the exact correspondence—or lack thereof—with those in patients with A-T, but we chose to focus this initial assessment on the cerebellar cortex.

Neuronal abnormalities, both subtle and gross, were detected at the electron microscopic level almost exclusively in

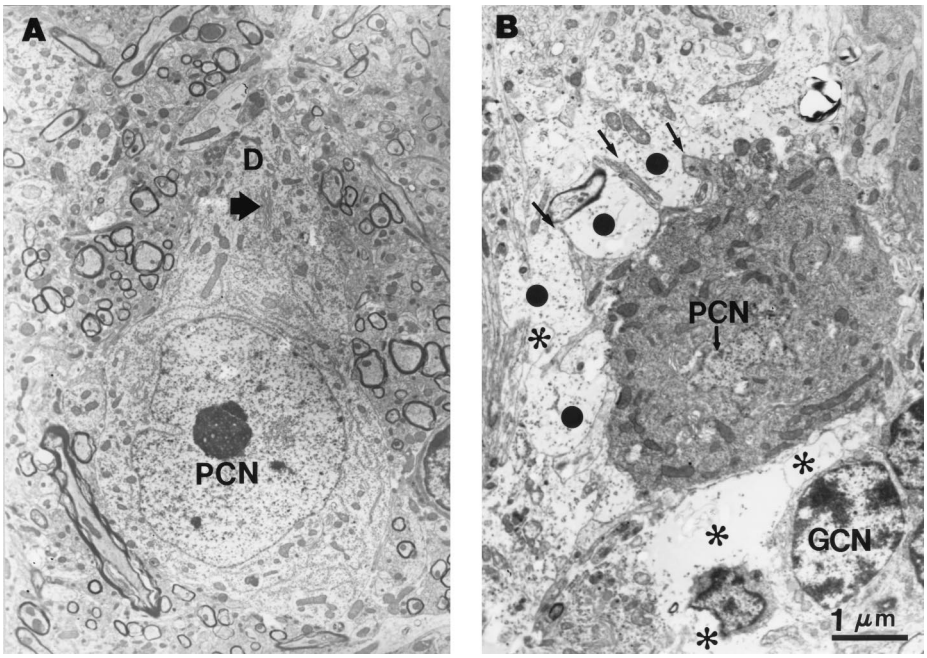

FIG. 1. (*A*) Electron micrographs of a normal Purkinje neuron in a control animal compared with a degenerating Purkinje cell in a knockout specimen (*B*). The degenerating neuron has both a crenated surface profile and nucleolemma, more electron dense cytoplasm, and filiform processes originating from its surface (arrows) and is surrounded by confluent vacuolated spaces (asterisks) and distended cell processes (large dots). These features are in contrast with the normal Purkinje neuron, which has a smooth perikaryal contour and nucleolemma, except for the single indentation of the latter, lighter cytoplasm, and a lesser density of mitochondria, and its processes, such as one dendrite (D), are much thicker. The control neuropil is also tight and full, lacking any significant interstitial spaces and distended processes surrounding the Purkinje neuron. PCN, Purkinje cell nuclei; GCN, granule cell nucleus. The arrow in *A* points to the Golgi apparatus. The magnification is the same in both panels.

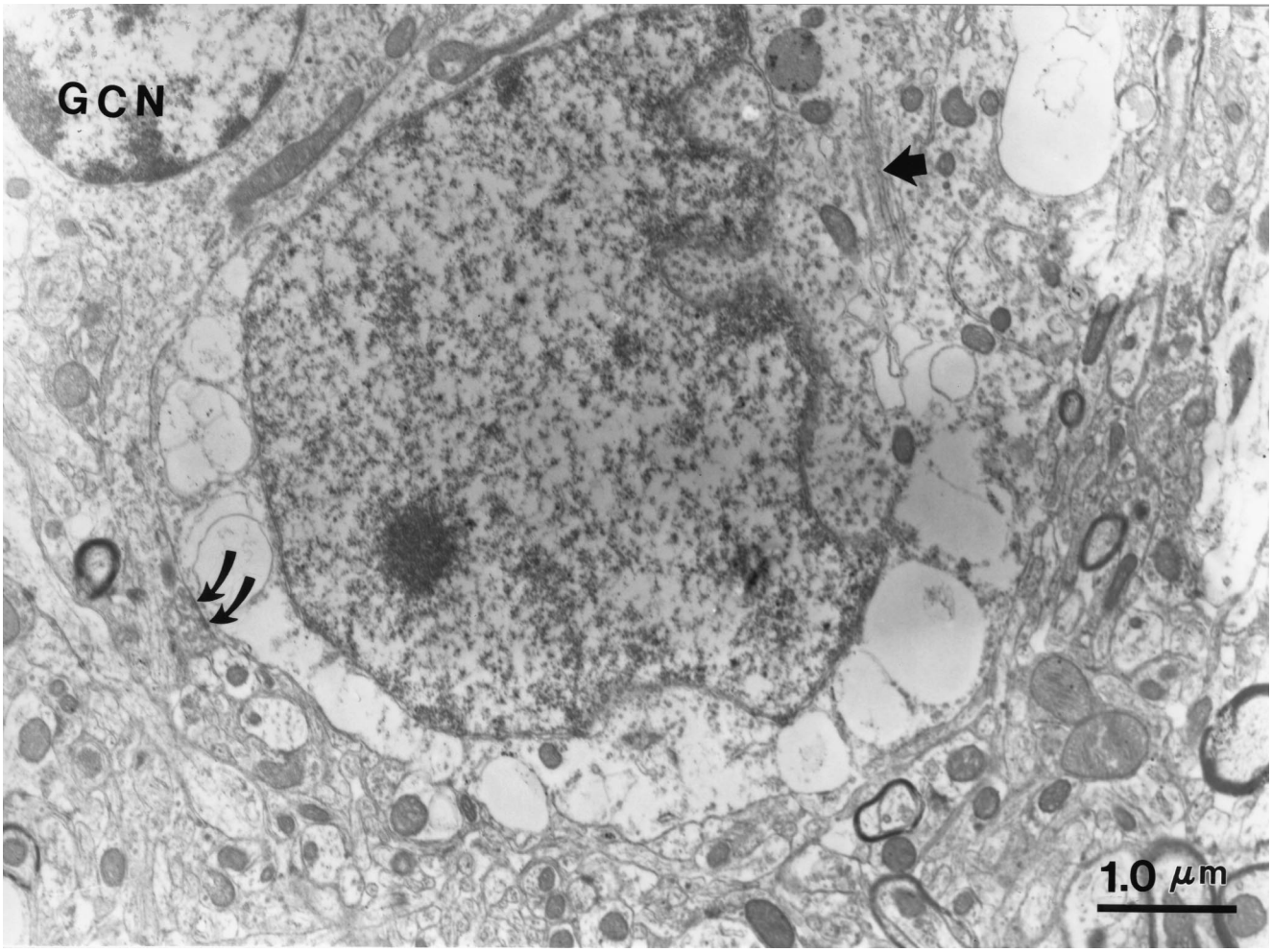

FIG. 2. Electron micrographs of a degenerating neuron identifiable by synapses on its surface (curved arrows) from an *Atm* knockout specimen. The synapses on the perikaryon, the clear, granular cytoplasm, the prominent, elongated Golgi apparatus, the lobulated nucleus with relatively homogeneous chromatin, and the prominent nucleolus are among the features that this cell shares with Golgi neurons in the normal cerebellum. However, this neuron presents multiple, often confluent vacuolations within the cytoplasm, indicating that it is undergoing a degenerative process. GCN, granule cell nucleus.

Atm knockout mice and not in controls. These lesions were abundant because they were present in 280 (25%) of 1102 neuronal profiles in knockout mice (Table 1). By contrast, a similar search for abnormal profiles in controls yielded only four (0.35%) abnormal cells among 1140. The lesions were distributed in the three layers of the cerebellar cortex, i.e., molecular, Purkinje cell, and granule cell layers. In controls, only three degenerating granule cells (0.3%) and one abnormal Purkinje neuron (1.5%) were found whereas knockouts had 180 (21%) degenerating granule cells, 33 (33%) abnormal Purkinje cells, and 67 (46.5%) degenerating neurons in the molecular layer. Obviously, these rough estimates ignore neurons that had already degenerated and presumably disappeared from the tissue because they were not available for counting.

Because Purkinje cell loss frequently has been observed in A-T, we focused first on this type of neuron. Control animals exhibit the well known morphological features of Purkinje cells, including a clear cytoplasm rich in mitochondria, with a well developed Golgi apparatus, a likewise pale nucleoplasm bound by a nucleolemma with a single or no indentation, and a dense, centrally situated nucleolus (Fig. 1*A*). Similar neurons also were found in knockouts, indicating that many Purkinje cells do not degenerate before the animals succumb from tumors. However, degenerating Purkinje cells can be easily identified, even on cursory examination of the material (Fig. 1*B*). These neurons most frequently exhibit a shrunken, crenated cell membrane from which filiform appendages originate, plus a darkened cytoplasm with an apparent increase in mitochondrial density, as well as a darkened nucleoplasm and a crenated nucleolemma. These obviously dystrophic Purkinje neurons are also surrounded by a mixture of distended cell processes resembling the terminals of basket cell axons that contact these neurons in normal specimens (large dots in Fig. 1*B*). These are interspersed with semiconfluent interstitial spaces that contain only some loose and disorganized membrane-like profiles that represent a significant loss of the texture of the neuropil (asterisks in Figs. 1, 3, and 4).

Degeneration is not restricted to Purkinje cells, however, because many other types of neuron (Figs. 2 and 3 *C* and *D*) and glial (Fig. 3 *A* and *B*) cells also exhibit dystrophic features in knockout animals. For example, interspersed among ubiquitous neuron-like degenerating profiles, other cells identified in previous studies as microglial cell bodies (19) appear to have a role in the creation of the abnormal interstitial spaces that result from the loss of the neuropil (Fig. 3 *A* and *B*). When small, these spaces are sparse and surround microglial cells, and the processes from these cells are insinuated around the walls of these spaces (Fig. 3*A*). In apparently more advanced stages of the same process, the microglial cell is suspended about the center of a vacuolated region of neuropil, after the individual cavities in the neuropil presumably have coalesced

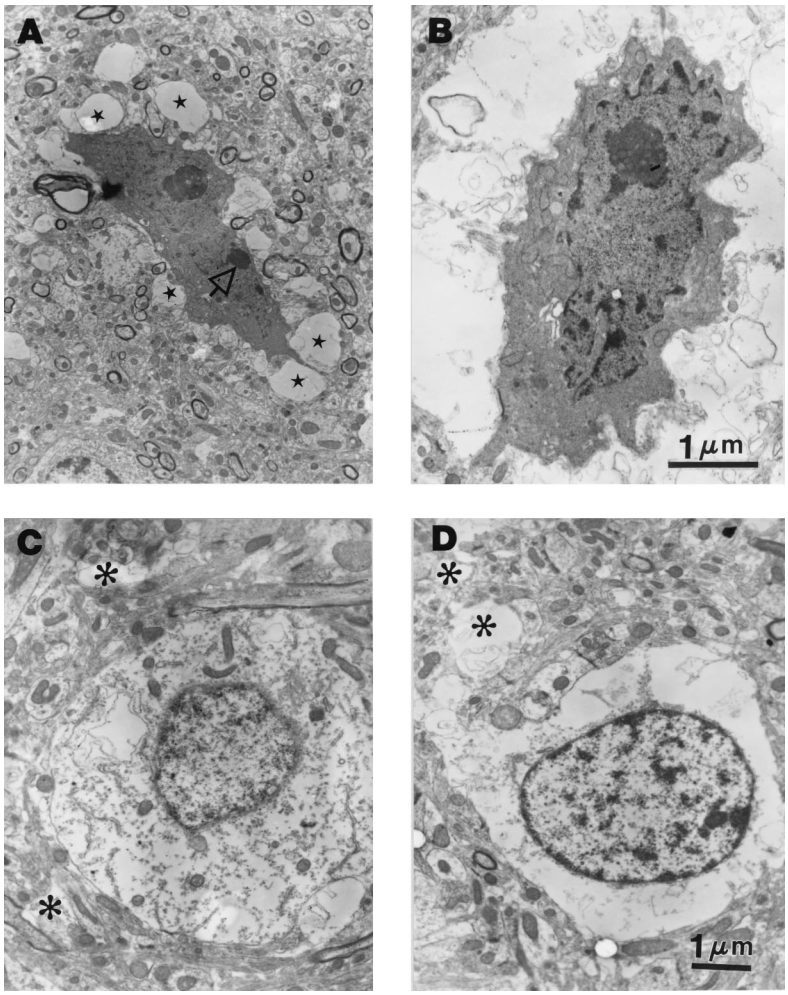

FIG. 3. Electron micrographs demonstrating microglial activation, neuropil disruption, and neuronal degeneration in an *Atm* knockout specimen. (*A* and *B*) represent two presumably consecutive phases of microglial activation associated with neuropil loss. Both panels contain a small elongated cell with numerous filiform appendages, a dark cytoplasm with lysosomes (arrow), crenated nucleolemma, and clumpy chromatin including a prominent nucleolus, i.e., features that have been correlated previously with microglia (cited in the text). Putative early stages are associated with vacuolations in the neuropil (stars) into which the filiform appendages of the microglial cells insinuate themselves (*A*). Presumably later stages are associated with much larger, lacune-like disruptions of the neuropil (*B*), which may result from the confluence of vacuoles such as those illustrated in *A*. *C* and *D* illustrate unequivocally degenerating neurons whose cytoplasm is severely disrupted, having lost most organelles, including mitochondria and the endoplasmic reticulum. Based on the morphological features of the normal cerebellum, the cell in *C* may be a Golgi neuron and that in *D* may be a granule neuron. Asterisks in *C* and *D* indicate vacuolations similar to those illustrated in Figs. 1 and 4, which may result from either the degeneration of the processes from the neuron in each panel or from the loss of nearby elements in the neuropil. Magnification in *A* and *C* as in *D*.

(Fig. 3*B*). In addition, neurons exhibiting various different ultrastructural features (i.e., resembling Golgi cells or granule cells) display a dramatic and unquestionably abnormal disintegration of their cytoplasm, with consequent loss of cytoplasmic organelles (Figs. 2 and 3 *C* and *D*). Apoptotic bodies were encountered occasionally but not invariably. In general, chromatin fragmentation and dissolution, and crenation of the nucleolemma, appeared as predominantly late phenomena because they were observed in cells with very advanced cytoplasmic alterations. The latter alterations, by contrast, tended to precede detectable structural alterations in the nucleus, yet this is an aspect that clearly needs very extensive quantitative analysis coupled with methods to assess nucleic acid breakdown in the future.

As might be expected, these ubiquitous abnormal features are accompanied by clear-cut evidence of degeneration in both pre- and postsynaptic elements (Fig. 4 *A–D*). In fact, many processes undergoing various stages of synaptic degeneration can be identified that still remain attached to a synaptic cleft (pointed at by curved arrows in Fig. 4 *A–D*), which in many cases have well preserved synaptic vesicles in the presynaptic elements (hollow arrows in Fig. 4 *A–D*). In the case of degenerating presynaptic terminals (Fig. 4 *A–C*), these are frequently distended and have lost most of their organelles and texture, with mostly loose membranes remaining, and the synaptic vesicles are clumped together, becoming darker than in normal terminals, near the active site of the synapse. Many degenerating postsynaptic elements are also distended and have lost their texture—like the preceding presynaptic terminals—yet can still be recognized unequivocally by the presence of a presynaptic terminal still attached to them and a postsynaptic density (Fig. 4*D*). Virtually all of these degenerating synaptic terminals occur near disrupted neuropil (asterisks in Fig. 4) and frequently in the proximity of profiles undergoing more advanced deterioration that appear to have also been synaptic contacts (e.g., DPrE? in Fig. 4*C*).

DISCUSSION

The preceding findings indicate unequivocally that *Atm* knockout mice exhibit widespread neuronal degeneration and glial activation, confirming the expectation that interference with

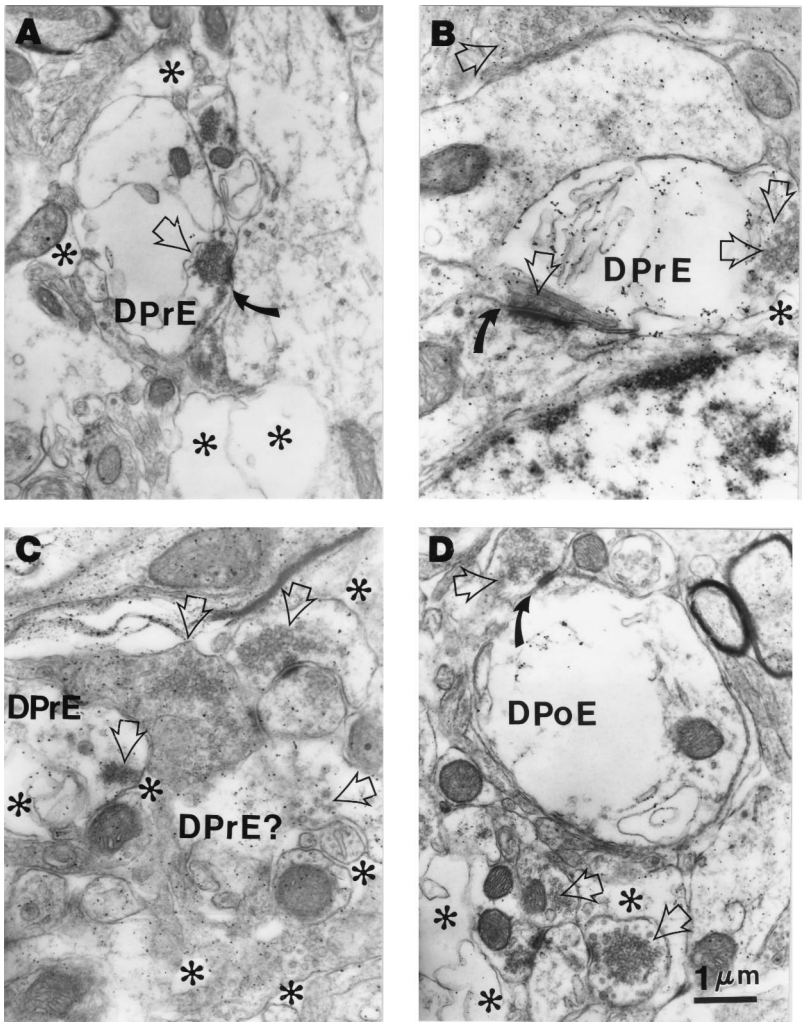

FIG. 4. Electron micrographs demonstrating degenerating pre- and postsynaptic elements (DPrE and DPoE, respectively) in an *Atm* knockout specimen, recognized by swelling, loss of cytoplasmic texture, and membrane-like remains in profiles participating in synaptic junctions recognized by their synaptic clefts (curved arrows) and, in the case of presynaptic elements (*A–C*), by some remaining synaptic vesicles (hollow arrows, used in all panels to highlight clusters of synaptic vesicles in both normal and degenerating profiles). Degenerating postsynaptic elements can be recognized by their associated synaptic clefts (curved arrow in *B*) to which a presynaptic profile containing synaptic vesicles (hollow arrow) is apposed. In addition to the pre- and postsynaptic degenerating profiles, all panels display an irregular, patchy loss of texture and disruption of the neuropil, which is scattered both around the degenerating profiles as well as around the nearby, otherwise apparently normal neuropil. The most severely disrupted neuropil is entirely devoid of protoplasm and organelles, containing only membrane-like remains, and is highlighted with asterisks in all panels.

Atm expression might result in A-T-like neurodegeneration. This is an important finding, given that previous lower resolution (i.e., light microscopic) analyses of all existing knockout mouse lines had failed to reveal any pathology, casting a premature doubt on the utility of *Atm* knockouts to study the neural aspects of A-T, even though these animals appeared to be useful models to study the nonneurological manifestations of this condition (13–15). There is another reason why the demonstration of lesions in the brain is indispensable to validate the utility of *Atm* knockouts as models of their human disease counterpart: Because the animals usually develop aggressive, rapidly growing tumors and die at ≈3 months of age, their systemic conditions interfere seriously with existing methodology to verify behavioral manifestations that may result from neurodegeneration. In fact, although behavioral abnormalities resembling ataxia have been claimed in at least one such model (14), many workers in this field remain skeptical of such claims, among other reasons because the alleged behavioral deficits could not be correlated with A-T-like pathology in the brain. Behavioral analysis in the knockout line that we have used is still underway, and it is therefore not known yet whether the lesions that we have observed do have behavioral consequences although the expectation is that they should. In any event, it is important to determine whether the behavioral impairments claimed to occur in other *Atm* knockout mice lines are associated with cerebral and, in particular, cerebellar degeneration similar to that described here.

Among the many questions that remain for analysis in this model, one of the key ones pertains to whether the neuronal degeneration is due to apoptosis or necrosis or both. Unfortunately, this question cannot be answered conclusively at this time because the present ultrastructural findings appear compatible with a mixture or combination of both processes. This is not surprising, once a considerable amount of degeneration is underway, because this presumably results in transneuronal degenerative phenomena that can obscure the original degenerative process, whichever it may be. The answer must await, therefore, further studies using a combination of light and electron microscopic observations in younger animals to determine whether the first neurons to degenerate undergo apoptotic or necrotic processes or perhaps both.

It is also necessary to determine whether other regions of the cerebellum (e.g., subcortical nuclei), other motor structures

(e.g., the olivary complex), and nonmotor regions that undergo degeneration in A-T (e.g., dorsal root ganglia) also are affected in *Atm* mice, precisely how do these changes correlate with those in actual patients, exactly how do they develop in the course of the life of the knockouts, and whether they correlate with any objective behavioral abnormalities. We therefore are attempting to suppress the thymic tumors in *Atm* −/− mice to prolong their lifespan and thus allow a longer time for the development of more advanced neurodegeneration and its likely behavioral concomitants. This task will necessarily be complicated by the relative lack of histopathological assessments of A-T with neuropathological methodology developed in the last decade and particularly by the paucity of electron microscopic characterization of the degeneration in this condition. Nevertheless, the present observations demonstrate that *Atm* knockout mice exhibit neurodegeneration similar—if not identical—to that described in A-T and, therefore, that they will become a useful tool to elucidate some of the mechanisms underlying the neurological manifestations of A-T. Ideally, the latter undertaking should include a detailed ultrastructural assessment of the other animal models of A-T and a parallel reassessment of the brain pathology in patients with this condition using current methodology to improve our understanding of the condition achieved in decades past.

We thank Dr. Galina Olennikova and Mrs. Juanita Johnson for contributing their skill in tissue processing. We also are grateful to Drs. Nancy S. Peress (S.U.N.Y. at Stony Brook), Carol K. Petito (University of Miami), Michael Norenberg (University of Miami), and Pasko Rakic (Yale University) for critical comments on drafts of this report. This work was supported by the A-T Children's Project, the United States Department of Veterans Affairs Merit Review Award 5065.01, the South Florida Veterans Affairs Foundation for Research and Education, National Institutes of Health and Public Health Service Grant NS 29856, and educational grants from the Eisai Corporation and Pfizer, Inc.

1. Louis-Bar, D. (1941) *Confinia Neurol.* **4,** 33–42.
2. Syllaba, L. & Henner, K. (1926) *Rev. Neurol.* **1,** 541–562.
3. Taylor, A. M., Metcalfe, J. A., Thick, J. & Mak, Y. F. (1996) *Blood* **87,** 423–438.
4. Harnsden, D. G. (1994) *Int. J. Radiat. Biol.* **66,** S13–S19.
5. Bundey, S. (1994) *Int. J. Radiat. Biol.* **66,** S23–S29.
6. Easton, D. F. (1994) *Int. Radiat. Biol.* **66,** S177–S182.
7. Leuzzi, V., Elli, R., Antonelli, A., Chessa, L., Cardona, F., Marcucci, L. & Petrinelli, P. (1993) *Eur. J. Pediatr.* **152,** 609–612.
8. Sedgwick, R. P. & Boder, E. (1991) in *Handbook of Clinical Neurology*, eds. Vinken, P., Bruyn, G. & Klawans, H. (Elsevier, Amsterdam), Vol. 16, pp. 347–423.
9. Vinters, H. V., Gatti, R. A. & Rakic, P. (1985) *Kroc Foundation Series* **19,** 233–255.
10. Strich, S. (1966) *J. Neurol. Neurosurg. Psychiatry* **29,** 489–499.
11. Aguilar, M. J., Kamoshita, S. & Landing, B. H. (1968) *J. Neuropathol. Exp. Neurol.* **27,** 659–676.
12. Savitsky, K., Sfez, S., Tagle, D. A., Ziv, Y., Sartiel, A., Collins, F. S., Shiloh, Y. & Rotman, G. (1995) *Hum. Mol. Genet.* **4,** 2025–2032.
13. Xu, Y., Ashley, T., Brainerd, E. E., Bronson, R. T., Meyn, S. M. & Baltimore, D. (1996) *Genes Dev.* **10,** 2411–2422.
14. Barlow, C., Hirotsune, S., Paylor, R., Liyanaga, M., Eckhaus, M., Collins, F., Shiloh, Y., Crawley, J. N., Ried, T., Tagle, D. & Wynshaw-Boris, A. (1996) *Cell* **86,** 159–171.
15. Elson, A., Wang, Y., Daugherty, C. J., Morton, C. C., Zhou, F., Campos-Torres, J. & Leder, P. (1996) *Proc. Natl. Acad. Sci.* **93,** 13084–13089.
16. Kuljis, R. O. (1997) *Ann. Neurol.*, in press.
17. Kuljis, R. O. & Rakic, P. (1989) *J. Comp. Neurol.* **280,** 393–409.
18. Peters, A., Palay, S. L. & Webster, H. (1991) *The Fine Structure of the Nervous System: Neurons and Their Supporting Cells* (Oxford Univ. Press, New York).
19. Palay, S. L. & Chan-Palay, V. (1974) *Cerebellar Cortex* (Springer, New York).
20. Eccles, J. C., Ito, M. & Szenthágothai, J. (1967) *The Cerebellum as a Neuronal Machine* (Springer, Berlin).